Molecular Dynamics Simulations of Oxidized and Reduced *Clostridium beijerinckii* Flavodoxin

Rik Leenders,* Wilfred F. van Gunsteren,‡ Herman J. C. Berendsen,§ and Antonie J. W. G. Visser*
*Department of Biochemistry, Agricultural University, Dreijenlaan 3, 6703 HA Wageningen, The Netherlands, ‡Laboratorium für Physikalische Chemie, ETH-Zentrum, CH-8092 Zürich, Switzerland, §Laboratory of Biophysical Chemistry, University of Groningen, Nijenborgh 4, 9747 AG Groningen, The Netherlands

ABSTRACT Molecular dynamics simulations of oxidized and reduced *Clostridium beijerinckii* flavodoxin in water have been performed in a sphere of 1.4-nm radius surrounded by a restrained shell of 0.8 nm. The flavin binding site, comprising the active site of the flavodoxin, was in the center of the sphere. No explicit information about protein-bound water molecules was included. An analysis is made of the motional characteristics of residues located in the active site. Positional fluctuations, hydrogen bonding patterns, dihedral angle transitions, solvent behavior, and time-dependent correlations are examined. The 375-ps trajectories show that both oxidized and reduced protein-bound flavins are immobilized within the protein matrix, in agreement with earlier obtained time-resolved fluorescence anisotropy data. The calculated time-correlated behavior of the tryptophan residues reveals significant picosecond mobility of the tryptophan side chain located close to the reduced isoalloxazine part of the flavin.

INTRODUCTION

Flavodoxins are small bacterial flavoproteins which function as low-potential electron-transfer proteins. Depending on the oxidation state of the flavin, flavodoxins can exist in different conformations (Mayhew and Ludwig, 1975; Watt et al., 1991). The nature of these conformational changes is difficult to derive from the crystal structure alone. Therefore, information on the dynamics of flavodoxin in its different oxidation states is required. The motional characteristics of flavin mononucleotide (FMN) in the protein matrix of oxidized (OX) and reduced (HQ) *Clostridium beijerinckii* flavodoxin have been studied earlier using time-resolved fluorescence anisotropy measurements (Leenders and Visser, 1991, 1992; Leenders et al., 1993a, b).

Our goal was to gain insight in the active site dynamics. The protein-bound flavin, comprising the active site of the flavodoxin, can exist in three different oxidation states of which the oxidized and fully reduced state have been shown to be fluorescent (Visser et al., 1987; Visser, 1989; Leenders and Visser, 1991, 1992; Leenders et al., 1993a, b). The active site dynamics can thus be examined using flavin fluorescence. An advantage for using the flavin chromophore is the fact that flavodoxin contains only one flavin residue per protein molecule, which may simplify the interpretation of experimentally obtained time-resolved fluorescence anisotropy data.

Computer simulations of macromolecular dynamics have been performed for over 15 years. Early molecular dynamics simulations of proteins were performed in vacuo, in the absence of solvent molecules (McCammon et al., 1977; Northrup et al., 1980; Levitt, 1981; Ichiye and Karplus, 1983; Levy, 1985; Åqvist et al., 1985, 1986; Henry and Hochstrasser, 1987). These vacuum simulations describe motional features of buried residues rather well (van Gunsteren and Karplus, 1982a; Harris and Hudson, 1991), but the dynamics of residues located near the protein surface are distorted by the vacuum effect (Axelsen et al., 1988; Chen et al., 1988; MacKerell et al., 1988). Inclusion of solvent molecules in the simulations improves the behavior of the latter residues resulting in realistic low-frequency collective motion of parts of the protein located at the periphery of the protein.

The results obtained with molecular dynamics (MD) simulations can be validated with different experimental studies and vice versa. The relation between these calculations and experiments can be illustrated with some examples. First, 2-dimensional nuclear magnetic resonance (NMR) measurements in combination with molecular dynamics simulations have been shown to be of great help in obtaining information about unresolved molecular structures (de Vlieg et al., 1986; van Mierlo et al., 1990a, b). The structure of the retinol binding apoprotein was determined in this way by using the related structure of the holoenzyme as a starting structure in the simulations (Åqvist et al., 1986). Secondly, Ichiye and Karplus (1983) showed that the fluorescence depolarization on the picosecond time scale of tryptophan residues of lysozyme could be calculated using the results of a molecular dynamics simulation. Because the resolution of the time-resolved fluorescence anisotropy experiments is limited to the picosecond time scale, only the effective zero-time anisotropies and/or fast decaying anisotropies with decay times in the picosecond range can be compared with the calculated values. Fluorescence anisotropy measurements can be related to the time correlation function, which describes the

Received for publication 18 October 1993 and in final form 20 December 1993.

Address reprint requests to Dr. A. J. W. G. Visser, Department of Biochemistry, Agricultural University, Dreijenlaan 3, NL-6703 HA Wageningen, The Netherlands. Fax: 011-31-8370-84801.

Abbreviations used: FMN, flavin mononucleotide; MD, molecular dynamics; SPC, simple point charge; rms, root mean square; OX, oxidized; HQ, hydroquinone or reduced.

0006-3495/94/03/634/12 $2.00

angular displacement of the emission transition dipole moment (Ichiye and Karplus, 1983). Comparison of MD calculations and fluorescence anisotropy decay measurements is normally limited to a few protein residues (e.g., tryptophans and tyrosines), but in case of flavodoxin an additional chromophoric group, the isoalloxazine ring system of the flavin, can be used.

In this study we performed molecular dynamics simulations of the active sites of oxidized and reduced flavodoxin in a solvent environment. The calculated characteristics of both oxidation states were compared with each other as well as with those obtained with time-resolved fluorescence measurements (Leenders and Visser, 1991, 1992; Leenders et al., 1993a, b).

COMPUTATIONAL PROCEDURE

MD simulations were carried out using the GROMOS package (van Gunsteren and Berendsen, 1987) on the Cray Y-MP4/464 computer at SARA Scientific Computing Services Amsterdam. The GROMOS force field involves terms for bond stretching, bond-angle bending, dihedral angle bending and improper dihedral angle bending interactions, and nonbonded terms describing the Van der Waals' and electrostatic interactions. No explicit hydrogen-bonding term was included because this interaction is accounted for by the nonbonded interactions (Reiher, 1985), but the van der Waals' repulsion properties of polar atoms were increased as compared with the normal repulsion parameters (Hermans et al., 1984). MD simulations of both oxidized and reduced flavodoxin were performed in order to obtain a more detailed insight in the role of flexibility of the active site of flavodoxins in case of a redox change. The x-ray coordinates for oxidized and semiquinone *clostridial* flavodoxin (Brookhaven structures 3FXN and 4FXN, respectively) have been determined with 0.19-nm and 0.18-nm resolution, respectively (Burnett et al., 1974; Smith et al., 1977). Comparison of the diffraction patterns from crystals of the semiquinone and fully reduced flavodoxin (Ludwig et al., 1971), 1D-NMR studies (James et al., 1973), and 2D-NMR studies (Leenders et al., unpublished data) showed that the tertiary structure of fully reduced *clostridial* flavodoxin is nearly identical with that of the semiquinone form. The coordinates of the two resolved crystal structures were used as starting conformations, where in reduced flavodoxin flavin atom N(1) was kept unhydrogenated in agreement with nuclear magnetic resonance studies (Vervoort et al., 1986). For oxidized flavin the standard GROMOS force field has been used. For reduced flavin the standard force field parameters were modified slightly, partitioning the resulting negative charge over the flavin atoms N(1) and O(2) (see Fig. 1). The partial charges used for atoms N(1), C(2), and O(2) were −0.635 q, +0.27 q, and −0.635 q, respectively. These partial charges were based on the results of molecular orbital calculations; they were incorporated as one charge group in the GROMOS topology.

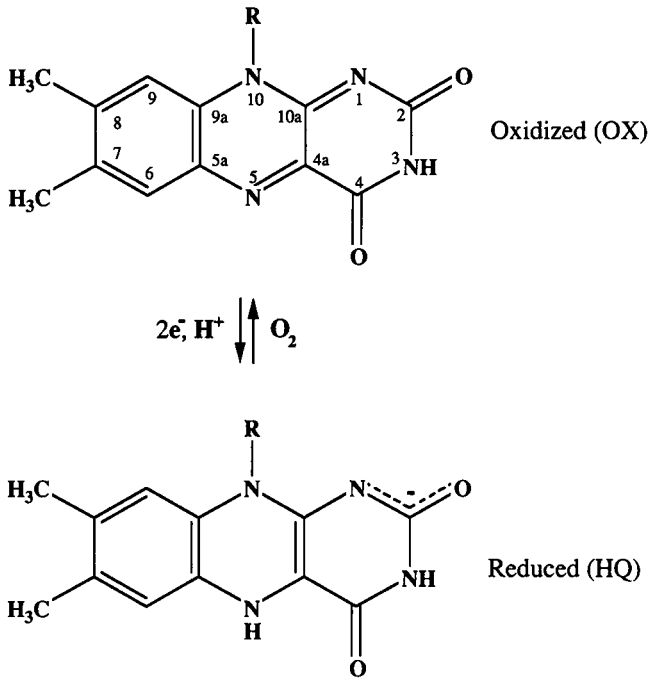

FIGURE 1 The molecular structure of oxidized and two-electron-reduced flavin mononucleotide (FMN). The molecule is composed of a isoalloxazine ring system and a ribityl side chain, *R* (-CH_2-(C(OH)H)$_3$-CH_2-O-phosphate). Upon reduction the protein-bound flavin atom N(1) remains unhydrogenated; the resulting negative charge is delocalized (see text).

Molecular topologies for oxidized and reduced flavodoxin were generated using the GROMOS residue topologies of RT37C and interaction function parameters of IFP37C4. In the GROMOS force field, hydrogens attached to nonpolar carbon atoms are incorporated in the latter forming united atoms, which reduces the required computer time significantly. Only the hydrogens able to form hydrogen bonds were included explicitly. Each flavodoxin was placed in a rectangular box filled with equilibrated simple point charge (SPC) water molecules (Berendsen et al., 1981). All solvent molecules that were positioned less than 0.23 nm from a flavodoxin atom were deleted. The best way to minimize edge effects caused by the vacuum is to use periodic boundary conditions, but because these simulations are still very computer intensive, only a solvent-sphere surrounding the active site has been simulated. The edge effects are then minimized by harmonically restraining the positions of the atoms in the outer shell of the protein-solvent system, whereas the atoms in the inner sphere are simulated without any positional restraints. In case of the simulations performed in this study, an inner sphere of 1.4 nm surrounding the center of the flavin chromophore was simulated without any positional restraint, whereas a shell of 0.8 nm (the atoms located between 1.4 nm and 2.2 nm from the flavin) was position-restrained to confine the shell-atoms to the simulation region (see Fig. 2). The force constant used for position-restraining was 10 kcal·mmol^{-1}·Å^{-2}). All residues that were partly located within the 1.4 nm sphere were totally included in the freely simulated region. Residues that are part

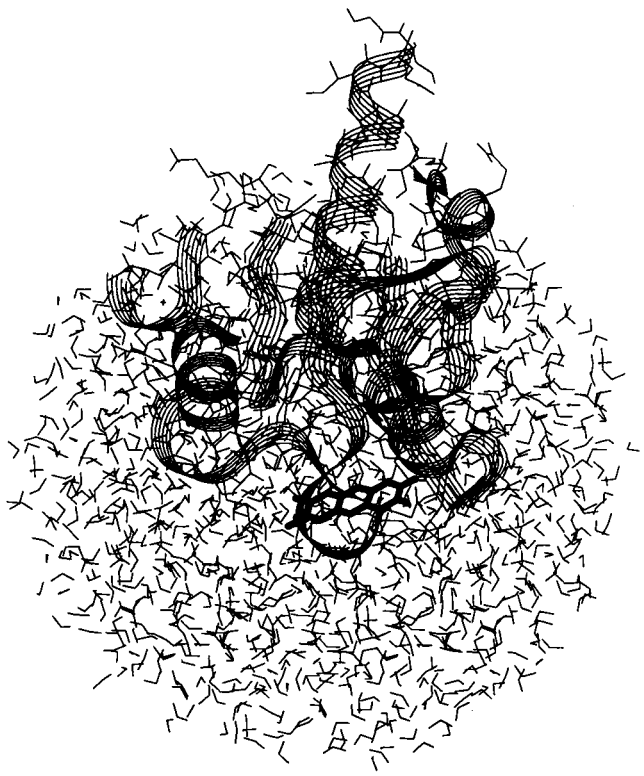

FIGURE 2 Schematic representation of a simulated system. The flavin isoalloxazine ring system is surrounded by a 2.2 nm sphere containing protein atoms and solvent molecules. The protein backbone is presented by a ribbon structure.

of the α-helix directed toward the negatively charged flavin phosphate are included in the simulation because of their supposed stabilizing effect (Hol et al., 1978). The radius of the inner sphere was chosen large enough to include the three tryptophan residues located close to the flavin, enabling a comparison of the simulated tryptophan behavior with experimental results (Leenders et al., to be published). The simulated systems consisted of 1034 protein (united) atoms with 1108 solvent molecules for the oxidized flavodoxin, and of 1027 protein atoms with 1090 solvent molecules for the reduced flavodoxin. For obtaining low-energy conformations, without local strain, the energy of the two systems was minimized for 100 steepest descent and 50 conjugate gradients steps. During energy minimization the solvent molecules located in the inner sphere were allowed to move freely, while the flavodoxin conformation was position restrained. The procedure was then repeated with the solvent molecules position-restrained and the flavodoxin atoms free. After this energy minimization no extra water molecules could be positioned indicating that a proper water density was achieved. The MD simulations were started by randomly assigning velocities (from a Maxwellian distribution) to the atoms yielding an overall kinetic energy corresponding to 300 K. Any residual transitional motion of and rotational motion about the center of mass was removed from the initial velocities to simplify analysis of the subsequent conformational fluctuations. The leap frog algorithm (Hockney and Eastwood, 1981) was used for integrating the equations of motion in cartesian coordinates. The SHAKE algorithm (Ryckaert et al., 1977; van Gunsteren and Karplus, 1982b) was used to constrain all covalent bonds allowing an integration time step of 2 fs. During the simulation the systems were coupled to an external bath with constant temperature (Berendsen et al., 1984), with temperature relaxation times of 0.1 ps. The systems were equilibrated until the total potential energy as well as the root mean square (rms) difference between the simulated structure and the initial x-ray positions remained constant. After these time points the coordinates, velocities, and energies were recorded every 25 steps (0.05 ps) until 375-ps trajectories were completed. Before analysis of the successive protein structures in the trajectories, a least squares fit was performed on the positions of the C(α) atoms. In the analyses only the freely simulated inner sphere of 1.4 nm is considered to avoid disturbing effects resulting from the applied position restraints or from the vacuum outside the simulated 2.2 nm sphere.

RESULTS AND DISCUSSION

Structure comparison and dynamics

Energy-minimization of the oxidized and reduced flavodoxins had reduced the potential energy to about $-3.3 \cdot 10^4$ kJ/mol. The molecular dynamics simulations were started and the total potential energy as well as the root mean square deviation between initial x-ray and MD-structure were monitored (van Gunsteren and Mark, 1992). The oxidized flavodoxin equilibrated within 60 ps, whereas the reduced flavodoxin reached equilibrium somewhat earlier (after 50 ps). The root mean square (rms) positional fluctuations, ΔR, were calculated according to:

$$\Delta R = \left[\frac{1}{N_{at}} \sum_{i=1}^{N_{at}} \langle \{(\Delta x_i)^2 + (\Delta y_i)^2 + (\Delta z_i)^2\} \rangle \right]^{1/2} \quad (1)$$

where Δx_i, Δy_i, and Δz_i are the differences between the instantaneous and averaged atomic coordinates for the i-th atom, the brackets ($\langle \cdots \rangle$) represent a time average, and the summation is over backbone and side chain atoms of the individual solute residues surrounding the center of the isoalloxazine ring system (inner 1.4 nm sphere). The backbone rms fluctuation, ΔR_B, averaged over C, O, C(α), and N atoms of the 51 residues located in the freely simulated inner sphere was almost identical for oxidized and reduced flavodoxin (ΔR_B is 0.037 and 0.041 nm, respectively), indicating quite rigid overall structures in both oxidation states (see Figs. 3A and 3C). This is in accordance with earlier results obtained with several spectroscopic techniques. From crystallographic studies (Burnett et al., 1974; Smith et al., 1977), it is known that *clostridial* flavodoxin has a compact structure with a central anti-parallel β-sheet embedded by four α-helices. Furthermore, two-dimensional NMR studies of the *clostridial* flavodoxin (Leenders et al., unpublished data) and the closely related *Megasphaera elsdenii* flavodoxin (van Mierlo et al., 1990a, b) showed that these flavodoxins have

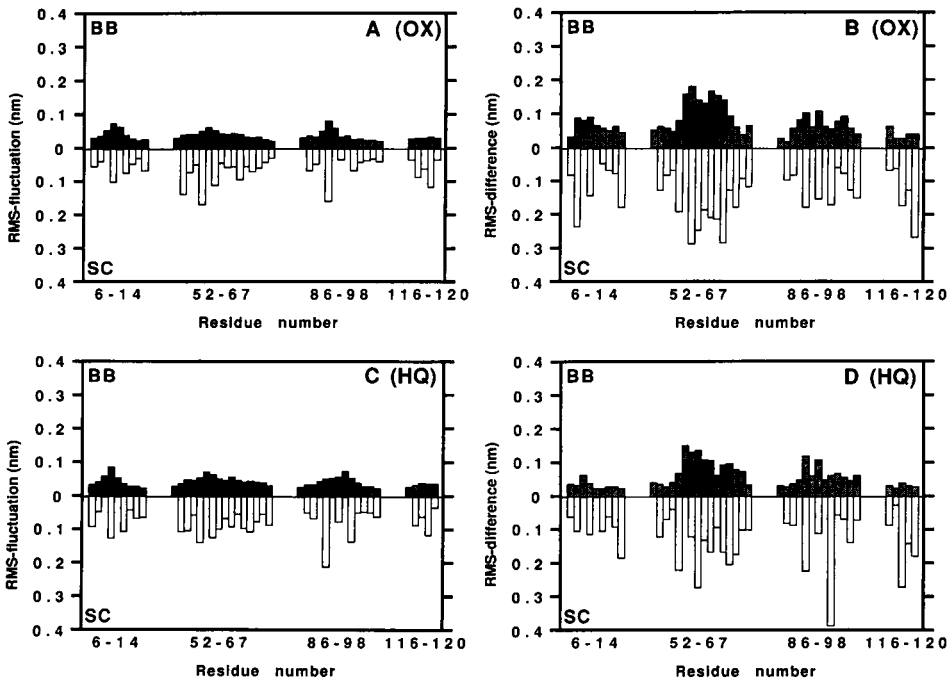

FIGURE 3 Rms fluctuations and differences for oxidized and reduced flavodoxin. *A*, rms fluctuations of oxidized flavodoxin (OX); *B*, rms difference between time-averaged and x-ray structure for OX; *C*, rms fluctuation of reduced flavodoxin (HQ); *D*, rms difference between time-averaged and x-ray structure for HQ. The values for backbone (BB) and side chain (SC) atoms are drawn with filled and open bars, respectively. Only the amino acids are presented of which both neighbors were simulated without any positional restraints.

compact structures without great fluctuations. The average rms fluctuation of the amino acid side chain atoms, ΔR_S, is somewhat larger than for the backbone atoms (Figs. 3A and 3C). For oxidized and reduced flavodoxin, ΔR_S was 0.058 nm and 0.073 nm, respectively. The absence of sterically hindering bulky side chains in the glycines adjacent to residue Trp90 combined with the fact that this tryptophan residue is located at the periphery of the protein result in large fluctuations of the tryptophan indole group in both oxidation states (Figs. 3A and 3C). This flexibility is examined in more detail in the section about tryptophan motional characteristics.

The rms fluctuation of oxidized and reduced flavin is 0.079 nm and 0.065 nm, respectively, and indicates that the flexibility of the protein-bound flavin is comparable with fluctuations of the backbone and side chain atoms of amino acid residues located in the vicinity of the chromophore. The magnitude of the flavin fluctuations does not appear to be influenced by less mobile amino acids that are part of α-helices and/or β-sheet. The rms fluctuations are distributed rather uniformly over the isoalloxazine ring system and ribityl side chain of both oxidized and reduced flavin. The only significant difference is found within the flavin phosphate group in the oxidized flavodoxin, which has higher rms fluctuations than the rest of the flavin. This behavior will be discussed later in some detail.

It is interesting to examine whether any correlation exists between the motional freedom of the flavin chromophore and the amino acids surrounding it. Therefore, atomic fluctuation cross-correlations were calculated using:

$$C(F, a) = \frac{\langle \Delta R_F \cdot \Delta R_a \rangle}{\langle (\Delta R_F)^2 \rangle^{1/2} \cdot \langle (\Delta R_a)^2 \rangle^{1/2}} \qquad (2)$$

where ΔR_F and ΔR_a is the (atomic) displacement from the mean position of the atoms of the flavin mononucleotide and amino acid residue, respectively. For both simulations three parts of the protein are found that show atomic fluctuations that are (positively) correlated with the flavin fluctuations (see Table 1); these regions are bound by residues 7 to 9, 54 to 60, and 87 to 89. The first region is part of the phosphate binding site, and the other residues are part of the isoalloxazine binding site. The correlations, which are found to propagate to approximately 1.1 nm in both oxidized and reduced flavodoxin, are always somewhat higher in reduced protein (see Table 1), except for residue Trp90. From the crystallographically obtained three-dimensional flavodoxin structures the side chain of residue Trp90 seems to be stacked to the isoalloxazine part of the flavin. However, from the simulation of oxidized and reduced flavodoxin, there is no sign of correlated motion of the two ring systems.

For oxidized and reduced flavodoxin the rms differences between the x-ray structure and the averaged MD structure are obtained using:

$$\Delta r = \left[\frac{1}{N_{at}} \sum_{i=1}^{N_{at}} (r_i^x - \langle r_i \rangle^{MD})^2 \right]^{1/2} \qquad (3)$$

where r_i^X and $\langle r_i \rangle^{MD}$ are the atomic position of atom i in the crystal structure and in the averaged MD structure, respectively, and the summation is over all atoms located in the 1.4-nm inner sphere. Figs. 3B and 3D show that the averaged MD structures of both oxidized and reduced flavodoxin have a high resemblance with their starting x-ray structures. The average rms differences of the backbone atoms, Δr_B, are 0.072 nm and 0.056 nm for oxidized and reduced flavodoxin, respectively. However, in both oxidation states the backbone of loop 57–63 has significantly higher average rms differences (Δr_B of about 0.15 nm) suggesting that this part of the

TABLE 1 Equal-time cross-correlations of the flavin chromophore positional fluctuations with those of amino acid residues in the oxidized and reduced flavodoxin*

Residue	C(OX)	C(HQ)	R_{av} (nm)	Residue	C(OX)	C(HQ)	R_{av} (nm)
Trp6	0.05	0.13	1.02	Gly86	0.08	0.07	1.02
Ser7	0.09	0.33	1.07	Ser87	0.10	0.26	0.67
Gly8	0.15	0.31	0.85	Tyr88	0.18	0.26	0.80
Thr9	0.10	0.30	0.86	Gly89	0.32	0.48	0.55
Gly10	0.15	0.13	1.02	Trp90	0.16	0.06	0.67
Asn11	0.29	0.11	0.87	Gly91	0.17	0.21	0.89
Thr12	0.10	0.21	0.92	Asp92	0.08	0.05	1.20
Glu13	0.09	0.17	1.31	Gly93	0.04	0.05	1.13
				Lys94	0.07	0.19	1.38
Gly52	0.06	0.07	1.30	Trp95	0.06	0.18	0.92
Cys53	0.00	0.04	0.94	Met96	0.04	0.10	1.26
Ser54	0.20	0.28	0.56				
Ala55	0.32	0.38	0.41	Val117	0.12	0.12	1.07
Met56	0.17	0.30	0.58	Gln118	0.18	0.24	0.97
Gly57	0.29	0.50	0.77	Asn119	0.14	0.19	0.73
Asp58	0.23	0.43	0.97	Glu120	0.05	0.14	1.10
Glu59	0.25	0.43	0.90				
Val60	0.20	0.27	0.96				
Leu61	0.08	0.08	1.14				

* The average distance, R_{av}, between amino acid and flavin chromophore calculated from both oxidation state is indicated.

protein has a solution structure that is different from the crystal structure. This difference is even larger for the side chains of these residues (Δr_S's more than 0.2 nm).

The average rms difference of the protein-bound flavin, Δr_F, is 0.104 nm and 0.145 nm for the oxidized and reduced flavin. Inspection of Fig. 4 shows that in the average simulated structures the oxidized flavin isoalloxazine ring system is translated and the reduced flavin ring system is somewhat rotated as compared with the initial x-ray structures. These findings were confirmed by comparison of the structures on a graphical display system. This slight rotation (of about 11°) could be a result of the choice of the charge partitioning on flavin atoms N(1) and O(2). However, because the apoprotein-to-flavin distances in the averaged MD structures are comparable with the distances in the solution structure of the related *M. elsdenii* flavodoxin (van Mierlo et al., 1990a), it is more likely that the flavin in the reduced flavodoxin has a solution structure that is slightly different from the initial x-ray structure. This could mean that the semiquinone and fully reduced flavodoxin have somewhat different active site conformations.

Comparison of the averaged MD structure of oxidized flavodoxin with that of fully reduced flavodoxin (data not shown) yields a backbone rms difference of 0.063 nm indicating that the overall structure of flavodoxin is more or less independent of its oxidation state (the backbone rms difference between the initial x-ray structures is 0.028 nm). The backbone atoms in specific regions have rms differences up to 0.2 nm (residues 56 to 64 and residues 90 and 91). The former difference is explained by the fact that in the reduced state the carbonyl of residue Gly57 is rotated toward the flavin as was demonstrated for the semiquinone state (Smith et al., 1977). This rotation is compensated by movement of backbone atoms located near residue Gly57. The latter difference is mainly the result of a change in backbone conformation near residue Trp90 in the simulated reduced flavodoxin.

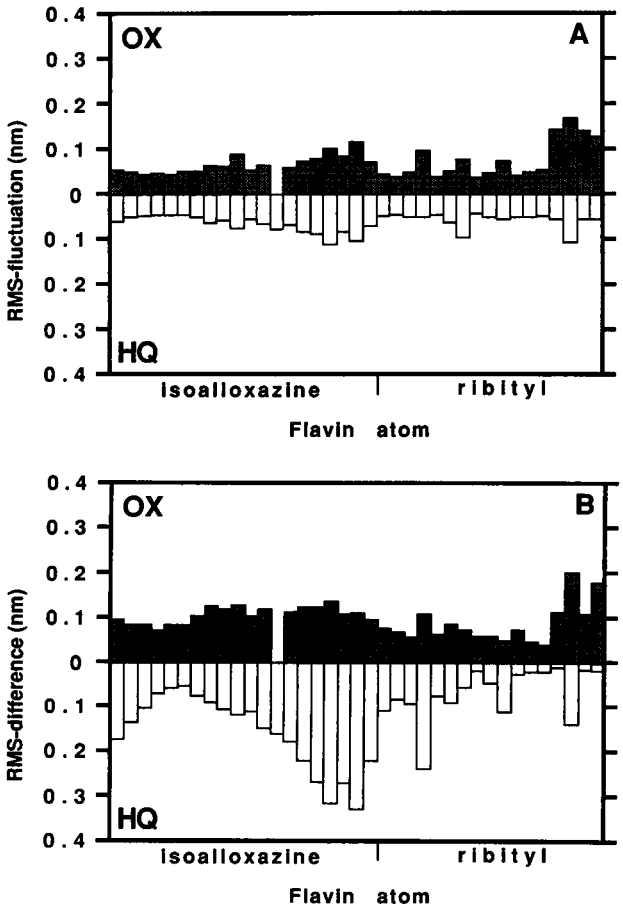

FIGURE 4 Rms fluctuations (*A*) and differences (*B*) of the oxidized and reduced protein-bound flavin (OX and HQ, respectively). Atom numbering is clockwise (see Fig. 1). The isoalloxazine atom sequence is C(9a), N(10), C(10a), N(1), C(2), O(2), etc. The reduced flavin contains one extra hydrogen (at position N(5)). The solvent accessible side of the reduced flavin ring system (the dimethyl ring) is somewhat shifted as compared with the position in the initial crystal structure.

The flavin rms difference between the averaged oxidized and reduced MD structures is 0.107 nm, which is of the order of the flavin rms difference between the initial crystal structures (0.073 nm). This means that the flavin as well as residues surrounding it occupy comparable positions in oxidized and reduced flavodoxin. The active site structure and dynamics of the flavodoxin in the oxidized and reduced state is examined in terms of hydrogen bonding patterns, dihedral angle transitions, solvent behavior, and flavin and tryptophan motional characteristics.

Dihedral angles

All active site dihedral angles (including the flavin dihedrals) of oxidized and reduced flavodoxin were monitored. As found earlier the solvent has a damping effect on the dihedral angle motion (van Gunsteren and Karplus, 1982a). The average backbone dihedral angles with their corresponding rms fluctuations are listed in Table 2. It is obvious that the backbone dihedrals show relatively small fluctuations, dihedral angle ω in particular. Attention was focused on dihedral angle transitions in order to locate regions with higher backbone flexibility. To define a transition, the dihedral angle has to cross the minimum between two adjacent dihedral potential wells. Furthermore, this transition should have a long enough lifetime. Because dihedral angle transitions occur typically in about 1 ps, an arbitrary choice for the minimum transition lifetime should at least be 2 ps. With this strict definition only a few backbone dihedral angle transitions occurred during the 375-ps trajectories.

In the oxidized flavodoxin 10 backbone dihedral angle transitions occurred involving dihedrals $\psi 9$ (backbone dihedral angle ψ of residue Thr9), $\phi 10$, $\psi 90$, $\phi 91$, whereas in the reduced flavodoxin only 2 short-lived transitions occurred that involved dihedrals $\psi 9$ and $\phi 10$. This is in accordance with the relatively high backbone rms fluctuations around these residues and results in different average backbone dihedral angles in these regions in oxidized and reduced flavodoxin. For example, dihedral angle $\psi 10$ in oxidized flavodoxin has an average value of 40.8°, whereas in reduced flavodoxin this dihedral is 5.2° (the rms fluctuations in this dihedral angle were similar in both oxidation states: 23.5° and 17.8°, respectively). Another significant difference is found at backbone dihedral angles near residue Trp90: $\phi 89$(OX) is −98.0° ± 17.1° and $\phi 89$(HQ) is −66.3° ± 16.5°; $\psi 90$(OX) is 9.9° ± 47.9° and $\psi 90$(HQ) is −34.0° ± 15.0°.

TABLE 2 Average backbone dihedral angles of oxidized (OX) and reduced (HQ) flavodoxin with their corresponding rms fluctuations*

	OX		HQ	
Dihedral angle	Average	rms	Average	rms
ω (C(α)-C-N-C(α))	177.9	5.4	178.6	5.5
ϕ (C-N-C(α)-C)	−79.8	9.6	−83.2	9.8
ψ (N-C(α)-C-N)	24.5	10.5	31.1	9.5

* The fluctuations were calculated similar to Eq. 1.

A similar large fluctuation as in $\psi 90$(OX) was found in the average dihedral angle $\phi 91$(OX): −105.9° ± 43.4°. The correlation between the fluctuations in dihedral angles $\psi 90$ and $\phi 91$ was calculated similar to Eq. 2. From the normalized cross-correlation coefficients, C(OX) is −0.94 and C(HQ) is −0.44, it can be concluded that these dihedral angles have fluctuations that are anticorrelated in both oxidation states, in particular in the oxidized flavodoxin. Another backbone dihedral angle differs considerably between the two simulated oxidation states: $\psi 57$(OX) is 99.9° ± 17.3° and $\psi 57$(HQ) is −114.1° ± 12.8°. This indicates that, although an extra hydrogen bond is formed upon reduction, this does not result in an altered mobility of this backbone dihedral angle of residue Gly57.

The flavin was also monitored for dihedral angle transitions. The only transition that occurred was of the ribityl side chain dihedral angle, C(ϵ)-O(ζ)-P-O. From this behavior it could be concluded that the phosphate group in the oxidized flavodoxin is bound more loosely than in the reduced protein, as was already demonstrated by the relatively high rms fluctuations of the atoms in the phosphate group. The dihedral angle switches between roughly two values: −60° and 60°. From the trajectories it can be calculated that in the oxidized state the value of this dihedral angle is −60° for 53% of the time, whereas in reduced flavodoxin this is 94%. This difference is also reflected in the difference in hydrogen bonding of the flavin phosphate with the apoprotein (Asn11); in oxidized flavodoxin this hydrogen bond exists for 50% of the trajectory and in reduced flavodoxin this is 91%.

This shows that in the active site region differences in both conformation and flexibility between the different oxidation states exist.

Intramolecular hydrogen bonding

From crystallographic studies of *Cl. beijerinckii* flavodoxin (Burnett et al., 1974; Smith et al., 1977) it is known which parts of the polypeptide chain surround the noncovalently bound flavin chromophore. It is also known that upon reduction of the flavodoxin the carbonyl group of residue Gly57 rotates toward the flavin atoms N(5) and H(5) (Smith et al., 1977). This indicates a role for one or more intramolecular hydrogen bonds influencing the motional behavior and characteristics of the isoalloxazine ring system in the reduced state. Therefore, the presence of hydrogen bonds during the simulations was investigated by scanning the 375-ps trajectories. The criteria for a hydrogen bond were taken as follows: the distance between hydrogen and acceptor atoms should be less than 0.25 nm and the angle between donor, hydrogen, and acceptor atoms has to exceed 135°. Hydrogen bonds involving flavin atoms in oxidized and reduced flavodoxin are listed in Table 3. From this Table it is obvious that both oxidized and reduced flavin are bound to the apoprotein by a large number of hydrogen bonds. An average overall number of hydrogen bonds can be calculated: the reduced flavin is bound by 14 H-bonds and the oxidized flavin by 11 H-bonds. The flavin phosphate group, which is

TABLE 3 Selection of hydrogen bonds involving flavin atoms, frequently occurring during the 375-ps simulation of oxidized (OX) and reduced (HQ) flavodoxins*

Donor	-	Acceptor	Donor	-	H	-	Acceptor	Occ_{OX}	Occ_{HQ}
Ser7	-	FMN	O(γ)	-	H(γ)	-	OT1	—	99
Gly8	-	FMN	N	-	H	-	OT1	37	10
Gly8	-	FMN	N	-	H	-	OH	—	87
Thr9	-	FMN	N	-	H	-	OH	37	10
Thr9	-	FMN	O(γ1)	-	H(γ1)	-	OT2	28	60
Gly10	-	FMN	N	-	H	-	OT2	42	54
Asn11	-	FMN	N	-	H	-	OT2	50	91
Thr12	-	FMN	N	-	H	-	OT1	16	91
Ser54	-	FMN	O(γ)	-	H(γ)	-	OT1	54	30
Glu59	-	FMN	N	-	H	-	O(4)	72	86
Gly89	-	FMN	N	-	H	-	N(1)	62	53
Gly899	-	FMN	N	-	H	-	O(2)	45	81
Trp90	-	FMN	N	-	H	-	N(1)	—	98
Gly91	-	FMN	N	-	H	-	O(2)	56	99
FMN	-	Ala55	O(β)	-	H(β)	-	O	56	—
FMN	-	Gly57	N(5)	-	H(5)	-	O	—	78
FMN	-	Ser87	O(δ)	-	H(δ)	-	O(γ)	79	91
FMN	-	Asn119	O(γ)	-	H(γ)	-	O(δ1)	15	—

* Occurrences less than 10% of the simulated time, are indicated (–).

surrounded by residues 8–12 and 54, is bound more firmly in the reduced flavodoxin as compared with the oxidized flavodoxin. The reduced flavin pyrimidine ring, surrounded by residues 59 and 89–91, is also bound in a more rigid manner than in oxidized flavodoxin as can be extracted from the hydrogen bonds involving flavin atom O(2) (Table 3).

The stability of the flavodoxin is indicated by the presence of a large number of (equivalent) hydrogen bonds within the oxidized and reduced apoprotein itself (data not shown). A selection of some differences in hydrogen bonding involving nonflavin atoms located in the freely simulated inner sphere is shown in Table 4. The protein structure, judging from analysis of all occurring hydrogen bonds, is nearly identical in the two oxidation states as was found when comparing the averaged atomic positions in both oxidation states.

Solvent behavior

In the dynamics calculations no information was included about specific protein-bound (crystal) water molecules. All solvent molecules were initially part of the bulk solvent. The solvent molecules located between 1.4 nm and 2.2 nm from the center of the flavin were position-restrained to minimize distortions, which are the result of the vacuum beyond the outer sphere. In the oxidized and reduced flavodoxin, 194 and 201 solvent molecules were simulated without any positional restraints (inner sphere). These solvent molecules show rms fluctuations ranging from 0.03 nm to 1.18 nm, indicating that some water molecules are almost immobilized, whereas others exhibit considerable motion. The overall solvent rms fluctuations are similar in both runs (ΔR_{sol} is 0.53 and 0.48 nm for the oxidized and reduced flavodoxin, respectively). The solvent molecules which have the smallest rms fluctuations are possibly bound to the protein, as some water molecules were demonstrated in the crystal structures of oxidized and semiquinone flavodoxin (Burnett et al., 1974; Smith et al., 1977). Therefore, the protein-solvent hydrogen bonding behavior was calculated from the 375-ps trajectories (we will call these interactions intermolecular).

The trajectories have been scanned for interactions between oxygen atoms in solvent molecules and any polar atom in the flavodoxin. The same criteria as for intramolecular hydrogen bonds were used. In both oxidation states some water molecules are located at close distance from the flavin during the entire run.

In the oxidized flavodoxin seven water molecules form hydrogen bonds with flavin atoms. During the span of the simulation, flavin atom N(3) forms hydrogen bonds with two water molecules that are both involved in other intermolecular hydrogen bonds (with the backbone oxygen of residue Trp90 and with the side chains of residues Asp58 and Glu59). The two hydrogen bonds between flavin atom N(3) and the two water molecules exist for 16% and 43% of the simulation time. The other five water molecules form hydrogen bonds with oxygen atoms of the ribityl side chain. In particular, atom O(γ) interacts with three different water

TABLE 4 Selection of hydrogen bonds involving nonflavin atoms which have large differences in occurrence between oxidized (OX) and reduced (HQ) flavodoxin

Donor	-	Acceptor	Donor	-	H	-	Acceptor	Occ_{OX}	Occ_{HQ}
Trp6	-	Glu65	N(ε1)	-	H(ε1)	-	O(ε1)	43	—
Ser7	-	Glu13	O(γ)	-	H(γ)	-	O(ε1)	99	—
Glu13	-	Ser7	N	-	H	-	O(γ)	—	72
Asp92	-	Glu59	N	-	H	-	O(ε2)	67	—
Asp92	-	Glu59	N	-	H	-	O(ε1)	59	—
Gly93	-	Glu59	N	-	H	-	O(ε1)	99	—
Lys94	-	Glu59	N	-	H	-	O(ε1)	99	—

molecules, one of which is bridged to the side chain of residues Asn11 (29%) and Asn119 (28%). In the crystal structure of oxidized flavodoxin, this water molecule is called W-2 (Burnett et al., 1974). The hydrogen bond involving the water molecule bridged to residue Asn119 exists for 42% of the simulation time, whereas the other two H-bonds occur 10% of the time. The latter water molecule and two other water molecules form hydrogen bonds with the ribityl phosphate group. One of these water molecules is not only bound to a oxygen atom of the phosphate group (43%) but is also bound to the side chain of residue Ser7 (65%) and the backbone nitrogens of residues Asn11 and Glu13 (28% and 99% of the time, respectively). This water molecule is called W-1 in the crystal structure of oxidized flavodoxin (Burnett et al., 1974).

In the reduced flavodoxin also seven water molecules are found to form hydrogen bonds with the flavin chromophore. Contrary to oxidized flavodoxin flavin atom O(2) is involved in a relatively strong hydrogen bond (present for 63% of the time) with a water molecule, which also interacts with the backbone nitrogen of residue Gly93 (19%). This water molecule is called W-3 in the crystal structure of semiquinone flavodoxin (Smith et al., 1977). Ribityl-side chain-atom O(β) forms a hydrogen bond with a water molecule (18%), which is also involved in H-bonds with residues Ser54 (26%) and Ala55 (13%). As in oxidized flavodoxin flavin atom O(γ) forms H-bonds with three water molecules (47%, 18%, and 10%) that are also bridged to the side chains of residues Asn11 (39%) and Asn119 (36%), and the backbone oxygen of Ala55 (11%). Two of these water molecules were demonstrated to be present in the crystal structure of semiquinone flavodoxin (W-2 and W-4). The flavin phosphate group in reduced flavodoxin is surrounded by three water molecules that form H-bonds for part of the simulation time (35%, 29%, and 21%, respectively). These water molecules also form hydrogen bonds with residues Thr9 (26%), Ser54 (25%), and Ala55 (22%). The water molecule involved in H-bonds with the flavin phosphate group and residue Thr9 is called W-1 in the crystal structure.

Although no crystallographic water molecules were incorporated explicitly in the initial structures, the simulations predicted all crystallographically determined waters correctly. Furthermore, some additional water molecules were demonstrated to form hydrogen bonds with the apoprotein during the simulation (*vide supra*). In contrast with what might be expected from the crystal structures the protein-bound water molecules are not bound all of the time. Generally, the strongest hydrogen bonds between water molecules and protein atoms exist for 40–50% of the time, but the majority of the protein-solvent hydrogen bonds is present for shorter periods indicating a dynamic active site, in which the noncovalently bound flavin chromophore is stabilized by a combination of interactions between flavin, protein, and solvent atoms.

Flavin and tryptophan motional characteristics

With time-resolved fluorescence depolarization measurements, the mobility of chromophores can be determined from the decay of the anisotropy:

$$r(t) = \frac{i_{\parallel}(t) - i_{\perp}(t)}{i_{\parallel}(t) + 2i_{\perp}(t)} \tag{4}$$

where $i_{\parallel}(t)$ and $i_{\perp}(t)$ are the fluorescence intensities polarized parallel and perpendicular with respect to the polarization direction of excitation. The anisotropy decay, $r(t)$, can be described by the time-correlation function of the reorientation of the emission transition dipole moment (Ichiye and Karplus 1983, and references cited therein):

$$r(t) = \tfrac{2}{5}\langle P_2[\hat{\mu}_a(0) \cdot \hat{\mu}_e(t)]\rangle\, e^{-t/\phi_r} \tag{5}$$

where the factor $\frac{2}{5}$ accounts for the maximum theoretical anisotropy as a result of photo-selection, $P_2[\cdots]$ is the second-order Legendre polynomial, $\hat{\mu}a(0)$ is the direction of the absorption transition moment at time $t = 0$ and $\hat{\mu}_e(t)$ is the direction of the emission transition moment at time t. These directions may be considered separately because light absorption occurs in about 10^{-15} s, which is much faster than the process of internal conversion ($\sim 10^{-12}$ s) before emission starts. The brackets, $\langle \cdots \rangle$, denote an ensemble average. Because overall rotational motion of the flavodoxin (with rotational correlation time ϕ_r) is on a different, much longer, time scale, Eq. 5 becomes:

$$r(t) = \tfrac{2}{5}\langle P_2[\hat{\mu}_a(0) \cdot \hat{\mu}_e(t)]\rangle \tag{6}$$

In case the $P_2[\cdots]$ correlation function reaches a plateau value the comparison between the results obtained with experiment and simulation are given to a good approximation by (Axelsen et al., 1988):

$$\langle P_2[\hat{\mu}_a(0) \cdot \hat{\mu}_e(t)]\rangle = P_2[\cos\delta] \cdot \langle P_2[\hat{\mu}(0) \cdot \hat{\mu}(t)]\rangle \tag{7}$$

where δ is the angle between the absorption and emission transition moments and is the direction of either the absorption or emission transition moment. The anisotropy can then be calculated by substitution of Eq. 7 in Eq. 6.

The direction of the absorption transition moments in the oxidized flavin chromophore is deduced from the work of Johansson et al. (1979). When calculating the P_2 correlation function, the emission transition moment was taken parallel with the first absorption transition moment (δ is 0°). From Fig. 5 it is evident that the P_2 correlation function reaches a plateau for both the oxidized and reduced protein-bound flavin. The high plateau values indicate that the flavin chromophore is more or less immobilized within the protein matrix. For reduced flavodoxin a plateau value was found that was somewhat higher ($P_2 = 0.95$). From the work of Leenders et al. (1993a), the angle δ between the absorption and emission transition moment in reduced clostridial flavodoxin was determined to be 30.1°. Substitution of these values in Eqs. 6 and 7 yields a calculated anisotropy of 0.250, in excellent agreement with the experimentally determined value of 0.249 ± 0.002 (Leenders et al., 1993a). Using the fact that angle δ is 10.5° in oxidized flavin (Leenders et al., 1990a; Bastiaens and Visser, unpublished results), the plateau value of $P_2 = 0.91$ corresponds with

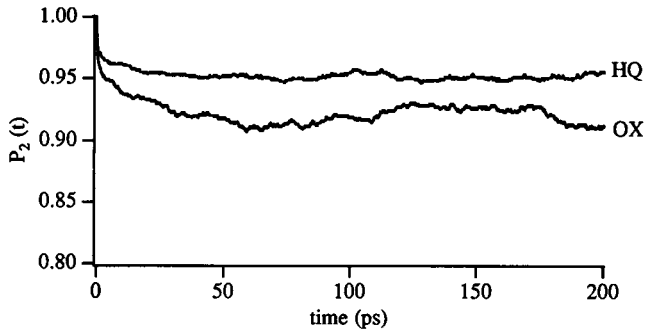

FIGURE 5 Time-correlation function $P_2(t)$ describing the reorientation of the first absorption transition dipole moment of oxidized (OX) and reduced (HQ) flavin. The orientation of the transition moment of reduced flavin is assumed to be identical with that of oxidized flavin (see text).

an initial anisotropy value of 0.346, which perfectly matches the experimentally determined initial anisotropy of 0.35 ± 0.01 (Leenders et al., 1993b). Because the calculated and experimentally determined initial anisotropies match very well, this confirms the motional rigidity of the protein-bound flavin as described by the dynamics calculations.

The simulation of the oxidized flavin did not reveal any nanosecond rotational motion as was demonstrated with fluorescence anisotropy measurements. This anisotropy decay component, which is thought to be an intermediate between the protein-bound and dissociated flavin chromophore, is an order of magnitude slower than the time scale of the calculations. Therefore, much longer simulations, without positional restraints within the protein matrix, would have to be performed to allow the noncovalently bound flavin to evolve to more loosely bound configurations.

Because the freely simulated inner sphere was chosen large enough, the three tryptophan residues were also allowed to undergo unrestrained motion. Analysis of the time correlation functions therefore can yield valuable information about the mobility of the tryptophan residues in a *pasteurianum* flavodoxin, because polarized fluorescence studies of tryptophan dynamics in flavodoxin have only been reported for *rubrum* class of flavodoxins (Leenders et al., 1990b). The location of the absorption moments in the molecular frame are known from earlier work (Yamamoto and Tanaka, 1972). To gain insight in the dynamic behavior of the tryptophan indole side chains, the $P_2(t)$ was calculated for the three tryptophans in the oxidized and reduced flavodoxins. From Fig. 6 it can be deduced that the three tryptophans have different motional freedom. In oxidized flavodoxin residue Trp6 shows slight motion on a long time scale, whereas residue Trp95 seems to be almost completely immobilized. Residue Trp90, however, shows a large motional flexibility. In reduced flavodoxin Trp95 is also immobilized. Residues Trp6 and Trp90 have significantly more motional freedom than in oxidized flavodoxin.

From the crystal structure it is known that the indole side chain of Trp90 and the isoalloxazine ring system of the flavin are coplanar. The differences in motional flexibility of residue Trp90 and the flavin chromophore, however, indicate that both residues have rather uncorrelated motion (this was already demonstrated in Table 1).

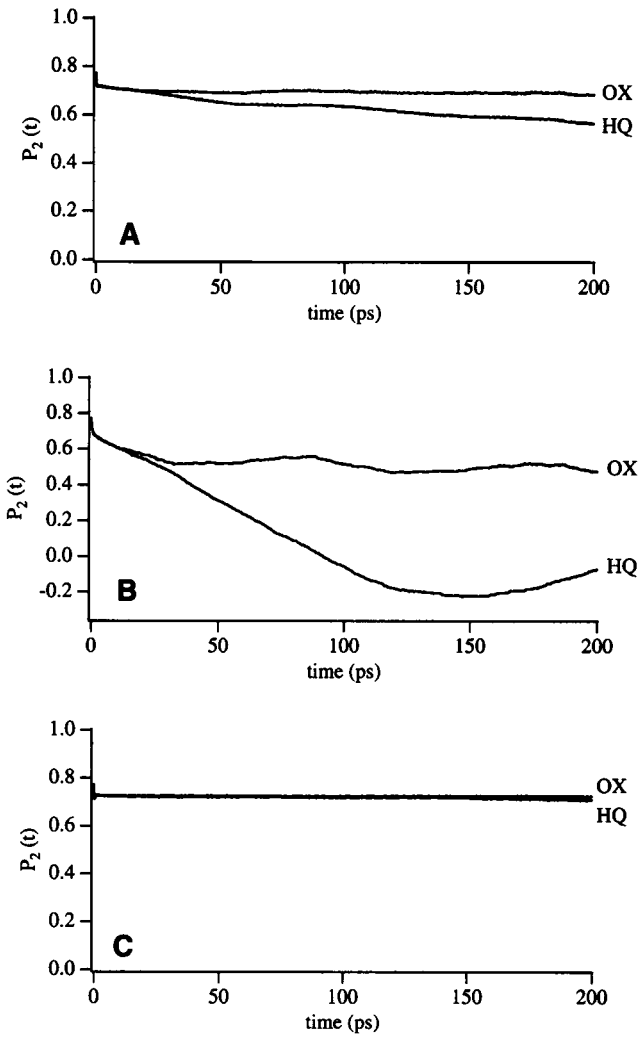

FIGURE 6 Time-correlation function $P_2(t)$ describing the reorientation of the ^1L_a absorption transition dipole moment of the three tryptophan side chain in oxidized and reduced flavodoxin. A limiting anisotropy of 0.31, corresponding to an angle $\delta = 22.8°$ (see Eq. 7), has been taken into account. A, Trp6; *B*, Trp90; *C*, Trp95. It is clear that residue Trp90 has considerable motional freedom, whereas residues Trp6 and Trp95 are bound more firmly (see text for details).

Tryptophan-to-flavin energy transfer

The three tryptophan residues and the flavin in the *clostridial* flavodoxin are separated by an average distance of about 1.2 nm. The interaction between the tryptophan residues and the flavin is monitored by calculating the Förster-type of energy transfer, which occurs due to dipole-dipole coupling. The rate of energy transfer from tryptophan donor to flavin acceptor, k_{ET} (in ns^{-1}), can be expressed by:

$$k_{ET} = \tau_{ET}^{-1} = (8.79 * 10^{17})\kappa^2 \frac{1}{\tau_R} R^{-6} J n^{-4} \qquad (8)$$

TABLE 5 The calculated κ^2/R^6 ratio averaged over the 7500 subsequent oxidized flavodoxin structures*

Donor	→	Acceptor	MD		X-ray	
			κ^2/R^6	τ_{ET} (ps)	κ^2/R^6	τ_{ET} (ps)
Trp6 (^1L_a)	→	FMN	0.679	15.3 ± 3.9	0.667	15.6
Trp6 (^1L_b)	→	FMN	0.040	247.0 ± 54.2	0.026	400.0
Trp90 (^1L_a)	→	FMN	13.108	0.79 ± 0.40	14.882	0.70
Trp90 (^1L_b)	→	FMN	170.91	0.06 ± 0.04	422.01	0.02
Trp95 (^1L_a)	→	FMN	0.807	12.9 ± 3.1	0.674	15.4
Trp95 (^1L_b)	→	FMN	0.081	128.0 ± 27.4	0.103	101.0

* The ratio for the initial crystal structure is given for comparison. The fluorescence lifetime, τ_{ET}, as a result of the tryptophan-to-flavin energy-transfer are also given (in ps). Errors are estimated from standard deviations in the κ^2/R^6 ratio and from the degree of uncertainty introduced by averaging the two *Desulfovibrio* overlap integrals. For details see text.

In this equation, τ_R is the (radiative) fluorescence lifetime of the tryptophan donor in the absence of the flavin acceptor, n is the refractive index of the medium between donor and acceptor, and J is the spectral overlap integral given by:

$$J = \int_0^\infty \frac{F(\nu)\epsilon(\nu)}{\nu^4}\, d\nu \qquad (9)$$

where $F(\nu)$ is the normalized fluorescence spectrum of tryptophan as a function of frequency ν, and $\epsilon(\nu)$ is the molar extinction coefficient of the flavin. The geometric parameters are the tryptophan-flavin center to center distance R (in nm), and κ^2, which is the orientation factor for the dipole-dipole interaction given by:

$$\kappa^2 = [\sin\theta_d \cdot \sin\theta_a \cdot \cos\zeta - 2\{\cos\theta_d \cdot \cos\theta_a\}]^2 \qquad (10)$$

Here ζ is the angle between the plane through the emission transition moment of the tryptophan donor and the separation vector and the plane through the second absorption transition moment of the flavin acceptor and the separation vector, and θ_d and θ_a are the polar angles made by these transition moments, respectively, with the separation vector.

Experimental measurements of tryptophan-to-flavin energy transfer involve averages over large ensembles of flavodoxin molecules. These results can be directly compared with those obtained from the simulations if the entire protein was simulated in a solvated state for a long period. The structural fluctuations of the flavodoxin would then be sampled with statistically significant frequencies. Because of computational limitations only the active site of the flavodoxin was simulated in a solvent sphere; however, the effects of internal motion upon the energy-transfer rates can be estimated from our calculations.

Because tryptophan has two potentially involved excited states, ^1L_a and ^1L_b, both rates of energy transfer to the flavin can be calculated. For the ease of calculation the location of the emission transition moments was taken parallel with the absorption transition moments determined by Yamamoto and Tanaka (1972), and the second flavin absorption moment in oxidized flavodoxin was taken from the work of Johansson et al. (1979). For reduced flavodoxin no exact location has been reported in literature for the latter transition moment. Therefore, energy transfer calculations can only be performed for oxidized flavodoxin.

Because R and κ^2 are the only variables in the ensemble, averaging over κ^2/R^6 is equivalent to averaging over k_{ET} (see Eq. 8). We calculated the values of κ^2/R^6 directly from the x-ray structure and compared these with the ones averaged over all subsequent MD-structures (see Table 5). It is obvious that the energy-transfer rates calculated for the crystal structure and the averaged MD-structure are unequal. Because the flavin ring system is relatively immobilized, this difference is mainly the result of dynamic effects of the tryptophan indole ring. Using the κ^2/R^6 ratio in combination with the radiative lifetime and the overlap integral the energy transfer rate can be calculated (Eq. 8). The radiative lifetime of tryptophan fluorescence was taken as 20 ns (Hochstrasser and Negus, 1984), and the refractive index was taken as 1.4 (Eisinger et al., 1969). The overlap integral was determined for the somewhat different *D. gigas* and *D. vulgaris* flavodoxins (Leenders et al., 1990b). Taking the overlap integral for *clostridial* flavodoxin as the average of the two *Desulfovibrio* overlap integrals (i.e., $0.84 \cdot 10^{-14}$ cm^3/M), energy-transfer times in the subpicosecond to subnanosecond range could be calculated (see Table 5). These values are in the order of the ones determined experimentally (Leenders et al., 1990b).

CONCLUSIONS

From the simulations it clearly follows that the overall active site conformation is similar in the averaged MD structures and the initial crystal structures. In particular, regions comprising α-helices and β-sheet have almost identical structures. However, regions with a somewhat altered conformation are also found. The backbone conformation of residues 57 to 63 shows rms differences of 0.15 nm (with side chains rms differences of up to 0.3 nm). These regions are located in the active site, near the flavin chromophore. The oxidized flavin only shows small rms differences, whereas the reduced flavin ring system has larger rms differences. This effect might be the result of the chosen charge separation for the nonprotonated atom N(1) in reduced flavin. The simulations further indicate that, on the time scale of the calculations, the flavin in oxidized as well as in reduced flavodoxin is immobilized in the protein matrix. The tryptophan residues have different motional flexibility. Residues Trp6 and Trp95 are almost immobilized, whereas residue Trp90, which is located at the periphery of the flavodoxin, has a large mo-

tional freedom, particularly in the reduced flavodoxin. This could be deduced from the large rms fluctuations of the Trp90 side chain atoms as well as from the fast decay of the P_2 time-correlation function. This flexibility may play a role in optimizing the electron transfer pathway to suitable electron acceptor proteins.

In vacuo simulations that have been performed earlier (data not shown) yielded anisotropies for the flavin that differed from the values found experimentally. Solvent inclusion mainly effects residues located at the periphery of the protein and is therefore necessary when comparing calculated and experimentally determined parameters, as was demonstrated when describing the motional behavior of the protein-bound flavin. In our simulations all initial solvent molecules were part of the bulk. No information about crystal water molecules was added. During the simulations the water molecules partitioned into two groups: solvent molecules in bulk with high rms fluctuations and solvent molecules which are protein-bound (small fluctuations). It was demonstrated that the latter solvent molecules are located similarly to the water molecules found in the crystal structures.

From fluorescence and fluorescence anisotropy experiments, it is sometimes very difficult to explain all the contributions in the decay profiles. From the simulations energy transfer rates could be calculated for the separate tryptophan residues. This is hardly possible in case of the experiments where one has to use proteins with selectively modified or changed residues.

In the case of flavodoxin, which has a compact and rigid structure, the use of spherical boundary conditions led to good results. However, one should keep in mind that spherical boundary conditions can only be used with considerable care, especially when little is known about dynamic properties of the protein under investigation.

We thank Dr. Jacob de Vlieg for his assistance in starting the molecular dynamics calculations. We also thank for the service provided by SARA Scientific Computing Services Amsterdam.

This work was sponsored by the Stichting Nationale Computerfaciliteiten (National Computing Facilities Foundation, NCF) for the use of supercomputer facilities, with financial support from the Nederlandse Organisatie voor Wetenschappelijk Onderzoek (Netherlands Organization for Scientific Research, NWO).

REFERENCES

Åqvist, J., W. F. van Gunsteren, M. Leijonmarck, and O. Tapia. 1985. A molecular dynamics study of the C-terminal fragment of the L7/L12 ribosomal protein. *J. Mol. Biol.* 183:461–477.

Åqvist, J., P. Sandblom, T. A. Jones, M. E. Newcomer, W. F. van Gunsteren, and O. Tapia. 1986. Molecular dynamics simulations of the holo and apo forms of the retinol binding protein. *J. Mol. Biol.* 192:593–604.

Axelsen, P. H., C. Haydock, and F. G. Prendergast. 1988. Molecular dynamics of tryptophan in ribonuclease-T1. *Biophys. J.* 54:249–258.

Berendsen, H. J. C., J. P. M. Postma, W. F. van Gunsteren, and J. Hermans. 1981. Interaction models for water in relation to protein hydration. *In* Intermolecular Forces. D. Pullmann, editor. Reidel, Boston. 331–342.

Berendsen, H. J. C., J. P. M. Postma, W. F. van Gunsteren, A. DiNola, and J. R. Haak. 1984. Molecular dynamics with coupling to an external bath. *J. Chem. Phys.* 81:3684–3690.

Burnett, R. M., G. D. Darling, D. S. Kendall, M. E. LeQuesne, S. G. Mayhew, W. W. Smith, and M. L. Ludwig. 1974. The structure of the oxidized form of clostridial flavodoxin at 1:9-Å resolution. *J. Biol. Chem.* 249: 4383–4392.

Chen, L. X.-Q., R. A. Engh, A. T. Brünger, D. T. Nguyen, M. Karplus, and G. R. Fleming. 1988. Dynamics simulations studies of apoazurin of *Alcaligenes denitrificans*. *Biochemistry* 27:6908–6921.

de Vlieg, J., R. Boelens, R. M. Scheek, R. Kaptein, and W. F. van Gunsteren. 1986. Restrained molecular dynamics procedure for protein tertiary structure determination from NMR data: a *Lac* repressor headpiece structure based on information on J-coupling and from presence and absence of NOE's. *Isr. J. Chem.* 27:181–188.

Eisinger, J., B. Feuer, and A. A. Lamola. 1969. Intramolecular singlet excitation transfer; applications to polypeptides. *Biochemistry* 8: 3908–3914.

Harris, D. L., and B. S. Hudson. 1991. Fluorescence and molecular dynamics study of the internal motion of the buried tryptophan in bacteriophage T4 lysozyme: effects of temperature and alteration of nonbonded networks. *Chem. Phys.* 158:353–382.

Henry, E. R., and R. M. Hochstrasser. 1987. Molecular dynamics simulations of fluorescence polarization of tryptophans in myoglobin. *Proc. Natl. Acad. Sci. (USA)* 84:6142–6146.

Hermans, J., H. J. C. Berendsen, W. F. van Gunsteren, and J. P. M. Postma. 1984. A consistent empirical potential for water-protein interactions. *Biopolymers* 23:1513–1518.

Hochstrasser, R. M., and D. K. Negus. 1984. Picosecond fluorescence decay of tryptophans in myoglobin. *Proc. Natl. Acad. Sci. (USA)* 81: 4399–4403.

Hockney, R. W., and J. W. Eastwood. 1981. Computer Simulation using Particles. McGraw-Hill, New York.

Hol, W. G. J., P. T. van Duijnen, and H. J. C. Berendsen. 1978. The α-helix dipole and the properties of proteins. *Nature* 273:443–446.

Ichiye, T., and M. Karplus. 1983. Fluorescence depolarization of tryptophan residues in proteins: a molecular dynamics study. *Biochemistry* 22:2884–2893.

James, T. L., M. L. Ludwig, and M. Cohn. 1973. Dependence of the proton magnetic resonance spectra on the oxidation state of flavodoxin from *Clostridium MP* and from *Peptostreptococcus elsdenii*. *Proc. Natl. Acad. Sci. (USA)* 70:3292–3295.

Johansson, L. B.-Å., Å. Davidsson, G. Lindblom, and K. Razi Naqvi. 1979. Electronic transitions in the isoalloxazine ring and orientation of flavins in model membranes studied by polarized light spectroscopy. *Biochemistry* 18:4249–4253.

Leenders, R., Ph. Bastiaens, R. Lunsche, A. van Hoek, and A. J. W. G. Visser. 1990a. Rotational resolution of methyl-group substitution and anisotropic rotation of flavins as revealed by picosecond-resolved fluorescence depolarization. *Chem. Phys. Lett.* 165:315–322.

Leenders, R., J. Vervoort, A. van Hoek, and A. J. W. G. Visser. 1990b. Time-resolved fluorescence studies of flavodoxin. Fluorescence decay and fluorescence anisotropy decay of tryptophan in *Desulfovibrio* flavodoxins. *Eur. Biophys. J.* 18:43–55.

Leenders, R., and A. J. W. G. Visser. 1991. Differences in flavin motional dynamics in oxidized and reduced *clostridial* flavodoxin as assessed by molecular dynamics simulations and fluorescence anisotropy. *In* Flavins and Flavoproteins. B. Curti, S. Ronchi, and G. Zanetti, editors. Walter de Gruyter, Berlin. 393–398.

Leenders, R., and A. J. W. G. Visser. 1992. Flavin dynamics in oxidized and reduced flavodoxins. *In* Time-Resolved Laser Spectroscopy in Biochemistry. Vol. 1640. J. R. Lakowicz, editor. Proceedings of SPIE-The International Society for Optical Engineering, Bellingham, Washington. 212–219.

Leenders, R., M. Kooijman, A. van Hoek, C. Veeger, and A. J. W. G. Visser. 1993a. Flavin dynamics in reduced flavodoxins. *Eur. J. Biochem.* 211: 37–45.

Leenders, R., A. van Hoek, M. Van Iersel, C. Veeger, and A. J. W. G. Visser. 1993b. Flavin dynamics in oxidized *Clostridium beijerinckii* flavodoxin as assessed by time-resolved polarized fluorescence. *Eur. J. Biochem.* 218:977–984.

Levitt, M. 1981. Molecular dynamics of hydrogen bonds in bovine trypsin inhibitor protein. *Nature* 294:379–380.

Levy, R. M. 1985. NMR relaxation and protein dynamics. *In* Proceedings of the Workshop on Molecular Dynamics and Protein Structure. J.

Hermans, editor. Polycrystal Book Service, Western Springs, Illinois. 62–64.

Ludwig, M. L., R. Andersen, P. A. Apgar, and M. LeQuesne. 1971. Preliminary crystallographic study of clostridial flavodoxin. *In* Flavins and Flavoproteins. H. Kamin, editor. University Park Press, Baltimore. 171–184.

MacKerell, A. D., L. Nilsson, R. Rigler, and W. Saenger. 1988. Molecular dynamics simulations of ribonuclease T1: analysis of the effect of solvent on the structure, fluctuations, and active site of the free enzyme. *Biochemistry* 27:4547–4556.

Mayhew, S. G., and M. L. Ludwig. 1975. Flavodoxins and electron-transferring flavoproteins. *In* The Enzymes (3rd Ed.). Vol. 12B. P. D. Boyer, editor. Academic Press, New York. 57–118.

McCammon, J. A., B. R. Gelin, and M. Karplus. 1977. Dynamics of folded proteins. *Nature* 267:585–590.

Northrup, S. H., M. R. Pear, J. A. McCammon, and M. Karplus. 1980. Molecular dynamics of ferrocytochrome c. *Nature* 286:304–305.

Reiher, W. E. 1985. Theoretical Studies of Hydrogen Bonding. PhD-thesis. Harvard University. Cambridge, Massachusetts. *Diss. Abstr. Int. B.* 47: 229–230.

Ryckaert, J.-P., G. Ciccotti, and H. J. C Berendsen. 1977. Numerical integration of the Cartesian equations of motion of a system with constraints: molecular dynamics of n-alkanes. *J. Comp. Phys.* 23: 327–341.

Smith, W. W., R. M. Burnett, G. D. Darling, and M. L. Ludwig. 1977. Structure of the semiquinone form of flavodoxin from *Clostridium MP*. *J. Mol. Biol.* 117:195–225.

van Gunsteren, W. F., and M. Karplus. 1982a. Protein dynamics in solution and in a crystalline environment: a molecular dynamics study. *Biochemistry* 21:2259–2274.

van Gunsteren, W. F., and M. Karplus. 1982b. Effect of constraints on the dynamics of macromolecules. *Macromolecules* 15:1528–1544.

van Gunsteren, W. F., and H. J. C. Berendsen. 1987. Groningen Molecular Simulation (GROMOS) Library Manual. Biomos, Groningen.

van Gunsteren, W. F., and A. E. Mark. 1992. On the interpretation of biochemical data by molecular dynamics computer simulation. *Eur. J. Biochem.* 204:947–961.

van Mierlo, C. P. M., Ph. Lijnzaad, J. Vervoort, F. Müller, H. J. C. Berendsen, and J. de Vlieg. 1990a. Tertiary structure of two-electron reduced *Megasphaera elsdenii* flavodoxin and some implications, as determined by two-dimensional ^{1}H NMR and restrained molecular dynamics. *Eur. J. Biochem.* 194:185–188.

van Mierlo, C. P. M., B. P. J. van der Sanden, P. van Woensel, F. Müller, and J. Vervoort. 1990b. A two-dimensional ^{1}H NMR study on *Megasphaera elsdenii* flavodoxin in the oxidized state and some comparisons with the two-electron reduced state. *Eur. J. Biochem.* 194:199–216.

Vervoort, J., W. J. H. van Berkel, S. G. Mayhew, F. Müller, A. Bacher, P. Nielsen, P., and J. LeGall. 1986. Properties of the complexes of riboflavin 3′,5′-biphosphate and the apoflavodoxins from *Megasphaera elsdenii* and *Desulfovibrio vulgaris*. *Eur. J. Biochem.* 161:749–756.

Visser, A. J. W. G., A. van Hoek, T. Kulinski, and J. LeGall. 1987. Time-resolved fluorescence studies of flavodoxin. Demonstration of picosecond fluorescence lifetimes of FMN in *Desulfovibrio* flavodoxins. *FEBS Lett.* 224:406–410.

Visser, A. 1989. Time-resolved fluorescence studies on flavins. *In* Fluorescent Biomolecules. D. M. Jameson, and G. D. Reinhardt, editors. Plenum Press, New York. 319–341.

Watt, W., A. Tulinsky, R. P. Swenson, and K. D. Watenpaugh. 1991. Comparison of the crystal structures of a flavodoxin in its three oxidation states at cryogenic temperatures. *J. Mol. Biol.* 218:195–208.

Yamamoto, Y., and J. Tanaka. 1972. Polarized absorption spectra of crystals of indole and its related compounds. *Bull. Chem. Soc. Jpn.* 45:1362–1366.